Crystal field parameters with Wannier functions: Application to rare-earth aluminates

P. Novák,* K. Knížek, and J. Kuneš
Institute of Physics of ASCR, Cukrovarnická 10, 162 00 Prague 6, Czech Republic
(Received 2 February 2013; revised manuscript received 5 April 2013; published 30 May 2013)

A method to calculate the crystal field parameters is proposed and applied to trivalent rare-earth impurities in yttrium aluminate and to Tb^{3+} ion in $TbAlO_3$. To determine crystal field parameters local Hamiltonian expressed in the basis of Wannier functions is expanded in a series of spherical tensor operators. Wannier functions are obtained by transforming the Bloch functions calculated using the density functional theory based program. The results show that the crystal field is continuously decreasing as the number of $4f$ electrons increases and that the hybridization of $4f$ states with the states of oxygen ligands is important. The method contains a single adjustable parameter characterizing the $4f$-ligand charge transfer. Theory is confronted with experiment for Nd^{3+} and Er^{3+} ions in the $YAlO_3$ matrix and for the Tb^{3+} ion in $TbAlO_3$, and a good agreement within a few meV is found.

DOI: 10.1103/PhysRevB.87.205139 PACS number(s): 71.70.Ch, 78.20.Bh, 71.15.Mb

I. INTRODUCTION

Ab initio calculations of the properties of molecules and solids have become a common tool of solid state physics and quantum chemistry. Nevertheless open problems remain, the description of the $4f$ states of rare-earth (R) elements being one of them. Above the Kondo temperature the physics of the $4f$ electrons is described by an effective atomic Hamiltonian. As the Kondo temperatures (with the exception of Ce or Yb compounds) of most rare-earth impurities are well below the experimental range of interest the effective atomic Hamiltonian provides an important tool to study the $4f$ physics. Parameters of the Hamiltonian may be fitted to experimental data or estimated using semiempirical or *ab initio* methods.

The original motivation of this work was to explain the magnetic properties of rare-earth cobaltites $RCoO_3$ (R = rare earth). For these compounds few experimental data are available, certainly not sufficient to estimate the crystal field parameters (CFP). Hence a necessity to calculate CFP emerged. To this end we have developed a method described in this paper. To check its reliability it was applied to orthorhombic rare-earth aluminates, possessing the same crystal structure as $RCoO_3$. Importantly, numerous experimental data exist for $R_xY_{1-x}AlO_3$, which are widely used in lasers, scintillator, and optical recording media. In several cases complete sets of CFP were deduced (see, e.g., Refs. 1 and 2).

The effective atomic Hamiltonian consists of the free ion interaction part $\hat{H}_A$ and the one-particle crystal field term $\hat{H}_{\rm CF}$

$$\hat{H} = \hat{H}_A + \hat{H}_{\rm CF}. \tag{1}$$

The rotationally invariant free ion Hamiltonian is only weakly material dependent. It contains the energy in a central field (a trivial constant when restricted to the $4f$ shell as usual), electron-electron interaction and the spin-orbit coupling. Details of $\hat{H}_A$ can be found in Ref. 3. Carnall *et al.*[4] determined the parameters of $\hat{H}_A$ for all R^{3+} ions in LaF_3 by carefully fitting the optical absorption spectra. The parameters for Nd^{3+} and Er^{3+} ions in $YAlO_3$[1] and for Tb^{3+} ion in $TbAlO_3$[2] were determined analogously.

Construction of the material specific $\hat{H}_{\rm CF}$ presents a formidable theoretical problem. The one-particle crystal field Hamiltonian can be written as[5]

$$\hat{H}_{\rm CF} = \sum_{k=0}^{k_{\rm max}} \sum_{q=-k}^{k} B_q^{(k)} \hat{C}_q^{(k)}, \tag{2}$$

where $\hat{C}_q^{(k)}$ is a spherical tensor operator of rank k acting on electrons in the $4f$ shell. $B_q^{(k)}$ are the crystal field parameters. For the f electrons $k_{\rm max}$ is equal to six, providing that cross terms of $\hat{H}_{\rm CF}$ between states of different angular momenta are neglected. Hermiticity of $\hat{H}_{\rm CF}$ requires that $B^k_{-q} = (-1)^q B^{k*}_q$.

The number of nonzero $B_q^{(k)}$ depends on the site symmetry. For a low site symmetry this number may be large and it is not *a priori* possible to predict, which of the CFP are important. When analyzing experimental data the CFP are usually determined by the least squares fit. This is often an ambiguous procedure with several equally likely solutions. In magnetic or superconducting compounds the number of experimental data is usually insufficient to determine CFP, yet the magnetic properties reflect the crystal field sensitively. There were therefore numerous attempts to estimate CFP theoretically and the effort is continuing (see Ref. 6 for recent survey).

In the present paper we use Wannier functions to construct the crystal field Hamiltonian. The method is applied to R^{3+} ions in orthorhombic aluminates. A detailed comparison with experimental data, presented in Sec. V, shows that the method is capable of an accurate prediction of the $4f$ crystal field parameters.

II. CRYSTAL FIELD STATES OF R^{3+} IONS IN ORTHORHOMBIC ALUMINATES

The orthorhombic rare-earth aluminates have a distorted perovskite structure belonging to the D_{2h}^{16} space group. The unit cell of $RAlO_3$ contains four formula units. The R sites with the point group C_s are surrounded by twelve oxygen atoms. Choosing the quantization axis along the orthorhombic c axis the horizontal symmetry plane causes all $B_q^{(k)}$ with odd q to be zero, leaving three real $B_0^{(k)}$ parameters ($k = 2, 4, 6$) and six independent complex parameters $B_q^{(k)}$ ($k = 2, 4, 6$; $q = 2, 4, 6$; $q \leqq k$). There are thus fifteen numbers to be determined. The spectrum of Hamiltonian [Eq. (1)] does not depend on its orientation with the respect to the crystallographic

axes. Therefore the imaginary part of a selected CFP can be eliminated by a specific rotation around the quantization axis,[7] and only fourteen independent CFP are needed to describe the experimental multiplet structures while the angle of rotation remains undetermined. Conventionally the $B_2^{(2)}$ parameter is set to be real. In the presented method all fifteen $B_q^{(k)}$ are determined. The rotation is only invoked in Sec. VI when comparing the calculated CFP with those obtained using the least squares fit by Duan *et al.*[1] and Gruber *et al.*[2]

On the one-particle level the C_s crystal field splits the seven $4f$ states $|l,m\rangle$ ($l = 3$, $m = \pm 3, \pm 2, \pm 1, 0$) into seven orbital singlets, which are of two different types. Four of these singlets are formed by $m = \pm 3$ and $m = \pm 1$ states; in the remaining three singlets $m = \pm 2$ orbitals are mixed with the $m = 0$ state. In our analysis instead of the $|l,m\rangle$ states the basis of real orbitals is used:

$$\begin{aligned}
|\varphi_1\rangle &= \frac{i}{\sqrt{2}}(|3,-3\rangle + |3,3\rangle) \sim y(3x^2 - y^2)\\
|\varphi_2\rangle &= \frac{1}{\sqrt{2}}(|3,-3\rangle - |3,3\rangle) \sim x(x^2 - 3y^2)\\
|\varphi_3\rangle &= \frac{i}{\sqrt{2}}(|3,-1\rangle + |3,1\rangle) \sim yz^2\\
|\varphi_4\rangle &= \frac{1}{\sqrt{2}}(|3,-1\rangle - |3,1\rangle) \sim xz^2\\
|\varphi_5\rangle &= \frac{1}{\sqrt{2}}(|3,-2\rangle + |3,2\rangle) \sim z(x^2 - 3y^2)\\
|\varphi_6\rangle &= \frac{i}{\sqrt{2}}(|3,-2\rangle - |3,2\rangle) \sim xyz\\
|\varphi_7\rangle &= |3,0\rangle \sim z^3.
\end{aligned} \tag{3}$$

In terms of real orbitals the wave functions of the seven singlets may be written as

$$\begin{aligned}
\psi_i &= \sum_{j=1}^{4} c_{j,i}\ |\varphi_j\rangle; \quad i = 1,2,3,4;\\
\psi_i &= \sum_{j=5}^{7} c_{j,i}\ |\varphi_j\rangle; \quad i = 5,6,7.
\end{aligned} \tag{4}$$

III. CALCULATION OF ELECTRONIC STRUCTURE AND DESCRIPTION OF METHOD

The computational procedure consists of two steps. The *initial step* of our analysis is the standard self-consistent solution of the Kohn-Sham equations of the density functional theory. Here we use the augmented plane waves + local orbital method implemented in the WIEN2K program.[8] For the exchange-correlation functional the generalized-gradient approximation form[9] was adopted. The experimental orthorhombic lattice parameters of $YAlO_3$[10] were used for $Y_{1-x}R_xAlO_3$ and $TbAlO_3$,[11] respectively, while the atomic positions within the unit cell were optimized for each system. The typical concentration x of R ions in $Y_{1-x}R_xAlO_3$ used as laser materials varies between 0.01 and 0.03. In our calculations the unit cell contained 120 atoms ($RY_{23}Al_{24}O_{72}$, corresponding to $x = 0.0435$) retaining the orthorhombic symmetry. The eigenvalue problem was solved in four points of the irreducible Brillouin zone, and the number of basis functions was ~9200 (corresponding to parameter $RK_{\max} = 6.13$). The calculations were non-spin-polarized and the $4f$ electrons were treated as *core* electrons, which contribute to the spherical component of the density only. As a consequence, the potential on the R site does not contain any nonspherical components arising from the on-site $4f$ states. This is vital for determination of the crystal field parameters, as otherwise the nonphysical interaction of the $4f$ states with the nonspherical potential they themselves create (self-interaction) would dominate CFP. Note that the core treatment of the $4f$ states is specific for the augmented plane waves basis and other methods require different means to eliminate the nonspherical part of the $4f$ self-interaction.

In the *second step* the effective crystal-field Hamiltonian for the $4f$ electrons is constructed from ingredients involving the shape of the $4f$ orbitals, the effective potential, and hybridization with the ligand orbitals. To this end the $4f(R)$ orbitals are included in the valence basis set. Before the eigenvalue problem with the potential from the initial step is solved the relative energy of the $4f$ and ligand states is modified by means of an orbitally dependent potential. This correction mimics the effect of electron-electron interaction within the $4f$ shell and we justify it as follows.

While the interatomic hopping parameters, determined largely by the orbital shapes and atomic distances, are relatively insensitive to the local Coulomb interaction, the energy separation of the $4f$ and ligand states is problematic. This is not surprising as we are trying to represent the physics of extremely correlated systems (the $4f$ shell) by an effective single particle scheme. There is no such universal representation. Instead, one can develop effective representations for specific quantities. For example, LDA + U provides such an effective model for one-particle photoemission and inverse photoemission spectra, i.e., transitions involving addition or removal of an electron. Here, we are interested in crystal-field optical excitations and thermodynamic properties, involving effects in which the number of electrons does not change. Therefore LDA + U is not applicable. The key quantity that controls the impact of the $4f$-ligand hybridization on the multiplet structure of the rare earth is the charge-transfer energy, the cost of moving an electron from the ligand to the $4f$ shell. The difference of the Kohn-Sham energies $\epsilon_f - \epsilon_p$ gives a poor estimate of the charge-transfer energy in a strongly interacting system. Therefore we introduce a correction Δ, which amounts to a downward shift of the oxygen s and p levels. The purpose of the correction is to modify the difference $\epsilon_f - \epsilon_p$ so that it approximates the actual charge transfer energy of the real material. We present more detailed reasoning in the Appendix. We eliminate the minor charge transfers (and corresponding level corrections) to other than oxygen orbitals by removing those from our basis set. The associated uncertainty of CFP is discussed in Sec. IV.

Once the eigenvalue problem is set up the remaining analysis reduces to algebraic manipulations. We proceed by transforming the Bloch states from the $4f$ energy window to Wannier functions using the wien2wannier interface[12] followed by standard application of the wannier90 software.[13] Wannier90 provides the seven by seven matrix $\hat{H}_{4f}$ of the Hamiltonian between the $4f$ Wannier functions centered on

the same atom, the traceless part of which is the desired crystal field Hamiltonian $\hat{H}_{\rm CF}$ (2)

$$\hat{H}_{4f} = E_{\rm avg}\hat{I} + \hat{H}_{\rm CF} = E_{\rm avg}\hat{I} + \sum_{k,q} B_q^{(k)}\hat{C}_q^{(k)}, \qquad (5)$$

where

$$E_{\rm avg} = {\rm Tr}(\hat{H}_{4f}/7). \qquad (6)$$

To get the CFP in the standard form we transform $\hat{H}_{4f}$ into the basis of spherical harmonics and expand it as a 49-dimensional vector in the basis of spherical tensor operators.

Summarized the computational procedure reads: (i) non-spin-polarized self-consistent WIEN2K calculation with $4f$ in core, (ii) solution of the eigenvalue problem with $4f$ in the valence window shifted with respect to the ligand states, (iii) construction of the Wannier functions for the energy window of the $4f$ states and extracting the on-site Hamiltonian, (iv) expansion of the on-site Hamiltonian in terms of the spherical tensor operators to obtain the CFP. We note that the concept of the local Hamiltonian is also in the heart of the CFP calculation method proposed recently by Hu *et al.*[14]

The method was first tested by determining the crystal field parameters of Pr^{4+} ion in PrO_2.[6] The results were similar to those reported by us earlier,[15] albeit without the uncertainty in decomposition of the density of states peaks. The symmetry of the Pr^{4+} site in PrO_2 is cubic and two real CFP are sufficient to characterize the crystal field. The $4f$ states are split in two triplets and singlet, and it is straightforward to determine CFP using the energy differences only. This, however, does not hold when the symmetry is lower: In orthorhombic aluminates the $4f$ states are split in seven singlets (4), and six energy differences are certainly insufficient to determine fifteen CFP. From the density of states projected on the $4f$ orbitals the orbital composition of the singlets, characterized by absolute values $|c_{ij}|$ in (4) may also be extracted, increasing the number of data obtained from DOS to 25. Our attempt to determine CFP using these data by the least squares led to similar ambiguity as encountered when analyzing the experimental results—several almost equivalent solutions were found. In contrast, the method based on decomposition of the local Hamiltonian gives the CFP set unambiguously.

IV. RESULTS

The calculations with the $4f(R)$ states in the core result in insulating band structures with the gaps ranging from 5.63 eV for R = Ce to 5.76 eV for R = Yb in $RY_{23}Al_{24}O_{72}$ and amounting to 5.04 eV in $TbAlO_3$. The valence band is dominated by oxygen $2p$ states, while the bottom of the conduction band is formed mainly by $5d(R)$ and $4d$(Y) orbitals. An example of the density of states from this calculation is shown in Fig. 1.

The density of one-particle states projected on Tb^{3+} $4f$ orbitals, obtained from the second step of our procedure is shown in Fig. 2. The overall strength of the crystal field may be characterized by the difference E_{cf} between the lowest and highest eigenvalues of the crystal-field Hamiltonian H_{cf} (see Fig. 2). The E_{cf} in $TbAlO_3$ is markedly bigger than the one in Tb:$YAlO_3$, indicating a large effect of the local geometry—in both cases this geometry was determined by minimizing the

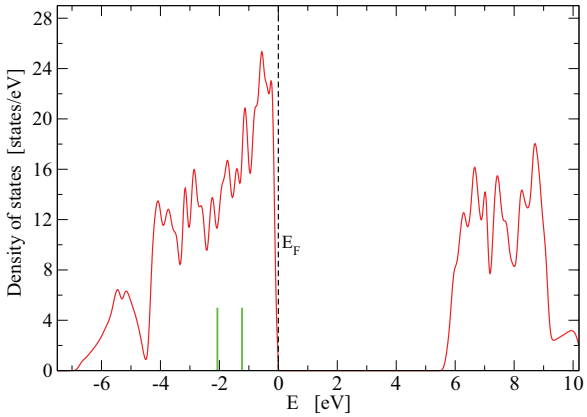

FIG. 1. (Color online) Total density of states of $TbY_{23}Al_{24}O_{72}$ with $4f$ states included in the core. Fermi energy is at zero, two vertical lines indicate the positions of $4f$ core levels, split by the spin-orbit coupling.

atomic forces. The dependence of E_{cf} on the number N_{4f} of the $4f$ electrons and for several values of Δ is shown in Fig. 3. As expected the effect of the f-p hybridization decreases with increasing $4f$-ligand level separation controlled by Δ. For fixed Δ the E_{cf} exhibits a monotonous dependence on the rare-earth element characterized by N_{4f}.

The full information about the crystal field in the form of the nonzero $B_q^{(k)}$ is shown in Figs. 4 and 5 using the typical value of $\Delta = -8.2$ eV. The dependence of $B_q^{(k)}$ on N_{4f} is again smooth, the largest term being $B_4^{(6)}$.

We remind the reader that the $4f$(R) states were allowed to hybridize only with the oxygen $2p$ and $2s$ states. For Er:$YAlO_3$ we have analyzed this approximation in detail. The eigenvalue problem was solved with the oxygen states shifted by $\Delta = -8.2$ eV and, in addition, the energy of a selected valence state (valence s, p, or d states of Er, Y, and Al) was left unshifted, thus allowing its hybridization with the $4f$(Er). The $4f$ energies were then compared with calculation in which the hybridization was prevented. The mean change of the $4f$ energy was in all cases smaller than 1 meV, with the exception of Er $5d$ states, where it reached 1.7 meV.

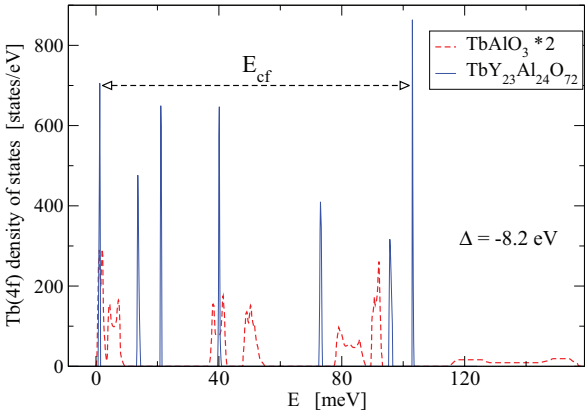

FIG. 2. (Color online) $TbAlO_3$ and Tb:$YAlO_3$. Density of states projected on the $4f$ subspace. The shift Δ equals to -8.2 eV. E_{cf} is the energy difference between the highest and lowest $4f$ singlet states and it is used to characterize the strength of the crystal field.

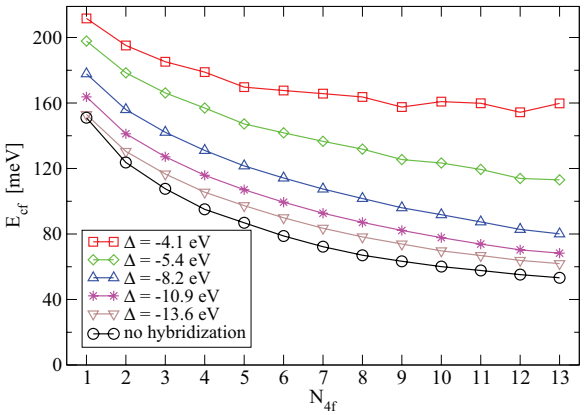

FIG. 3. (Color online) R:YAlO$_3$. The difference E_{cf} of the lowest and highest $4f$ eigenenergy across the lanthanide series for several values of Δ. The curves in this, as well as in the following figures, serve as guides for the eyes only.

V. COMPARISON WITH EXPERIMENT

In order to establish how well the calculated CFP describe the actual materials we have calculated the crystal field splitting of the $4f^n$ atomic multiplets in TbAlO$_3$, Nd:YAlO$_3$, and Er:YAlO$_3$, for which detailed experimental data exist.[1,2] To this end we have solved the eigenvalue problem for the effective Hamiltonian (1) using the "lanthanide" code.[16] To treat the different R^{3+} ions on the same footing we used the atomic parameters ($\hat{H}_A$) of Carnall *et al.*[4] Using alternative sets of the atomic parameters[1,2] led to marginal changes of the results.

In Fig. 6 the crystal field splittings of the Tb^{3+} seven lowest multiplets are compared to the experimental data.[2]

A similar plot for the Nd^{3+} in YAlO$_3$ is presented in Fig. 7. In this case the results are more sensitive to the value of Δ and calculations for $\Delta = -5.4$, -8.2, and -10.9 eV are confronted with the experiment.[1,17] In addition the results obtained with f-p hybridization completely eliminated are also included. As a third example we consider Er^{3+} ion in YAlO$_3$. As seen in Fig. 8 the experimental data for the four lowest multiplets are in a very good agreement with the calculation for Δ equal to -8.2 eV. To quantify the agreement between the theory and all

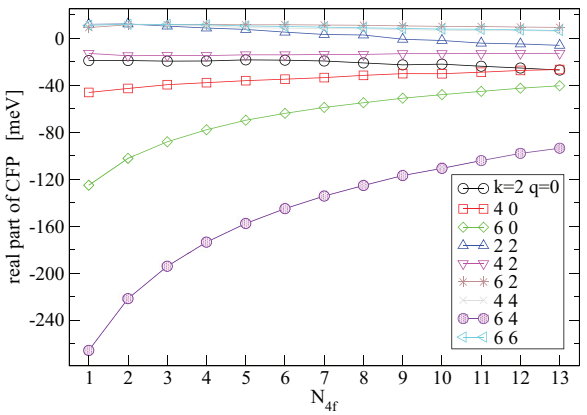

FIG. 4. (Color online) R:YAlO$_3$. Dependence of real part of the crystal field parameters on the number of $4f$ electrons. Shift $\Delta = -8.2$ eV.

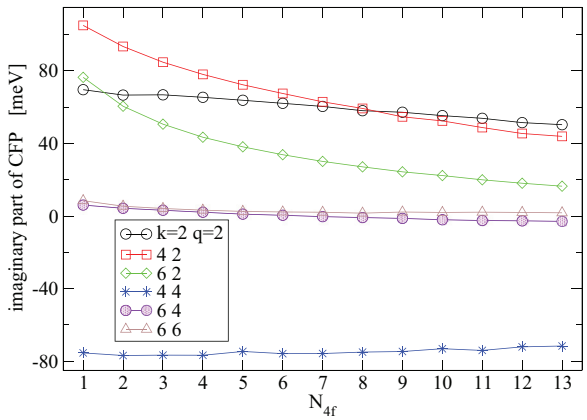

FIG. 5. (Color online) R:YAlO$_3$. Dependence of imaginary part of the crystal field parameters on the number of $4f$ electrons. Shift $\Delta = -8.2$ eV.

available experimental multiplet data without overloading the reader with information we have evaluated the mean square deviation of the experimental and calculated splittings:

$$\sigma = \sqrt{\frac{\sum_{j=1}^{n_{\rm exp}} (E_{j,\rm exp.} - E_{j,\rm calc.})^2}{n_{\rm exp}}}\,, \qquad (7)$$

where $n_{\rm exp}$ corresponds to the $|L,S,J\rangle$ multiplets, with the exception of the set 14, which combines $^2K_{13/2}$, $^2P_{1/2}$, and $^4G_{5/2}$ multiplets. The mean square deviation in Fig. 9 for the 19 lowest Er^{3+} sets indicates a good agreement between the experiment and theory with the exception of sets 14, 16, and 19. As shown in the figure not all levels were observed in these three cases, while for the remaining 16 multiplets the experimental information is complete.

VI. DISCUSSION

The results presented in Figs. 2, 6, and 7 show convincingly that the $4f$-ligand hybridization is important amounting to about 30% of the observed crystal-field splitting. The magnitude of our empirical estimates of Δ in the range 5–8 eV (Nd), 8–11 eV (Tb), and around 8 eV (Er) agrees with the experimentally observed trend of the charge-transfer

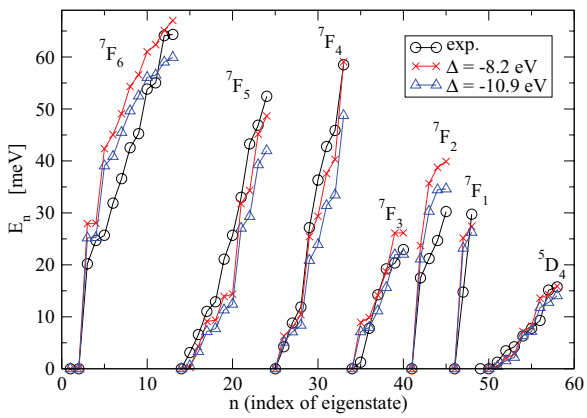

FIG. 6. (Color online) TbAlO$_3$. Energies of Tb^{3+} eigenstates taken relative to the lowest energy of the multiplet. The experimental data were determined by Gruber *et al.* (Ref. 2).

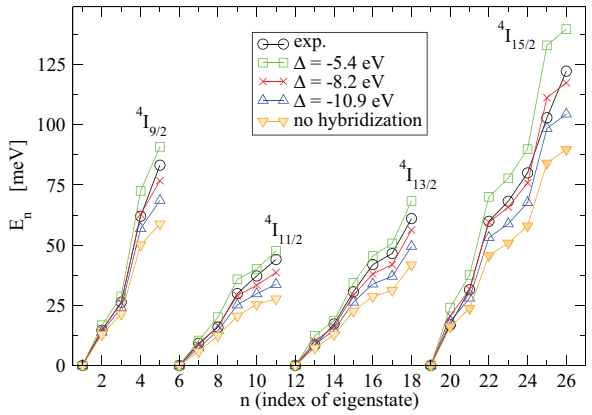

FIG. 7. (Color online) Nd:$YAlO_3$. Energies of Nd^{3+} eigenstates taken relative to the lowest energy of the multiplet. The experimental data were determined by Kaminskii (Ref. 17) and Duan *et al.* (Ref. 1).

energies[19] and reflects the strong Coulomb repulsion with the $4f$ shell.[20]

To compare the calculated CFP with those obtained by least squares fit to the optical spectra[1,2] we have to use the coordinate system in which $B_2^{(2)}$ is real as in the experimental analysis. This is achieved by rotation about the c axis by an angle $\alpha = -\text{arctg}(\text{Im}B_2^{(2)}/\text{Re}B_2^{(2)})$. The value of $\text{Im}B_2^{(2)}$ is large and positive for all R^{3+} ions, while $\text{Re}B_2^{(2)}$ is small and positive for lighter R, changing its sign for $R = \text{Dy}$ (see Figs. 4 and 5 for $\Delta = -8.2$ eV). The resulting α vs N_{4f} is shown in Fig. 10. The $\alpha(N_{4f})$ changes the sign, which leads to a discontinuity of the rotated $B_q^{(k)}(N_{4f})$ dependence despite the fact that in a fixed coordinate system the CFP change continuously with N_{4f}. This involves all the terms with $q = 2$ and $q = 4$. It is thus more informative to compare the absolute values of $B_q^{(k)}$ than their real and imaginary parts separately. Such a comparison for Nd^{3+} and Er^{3+} ions in $YAlO_3$ and for Tb^{3+} ion in $TbAlO_3$ is presented in Table I. The largest contribution comes from the $B_4^{(6)}$ term, and the crystal field decreases with an increasing number of $4f$ electrons. The CFP determined from the optical spectra suffer

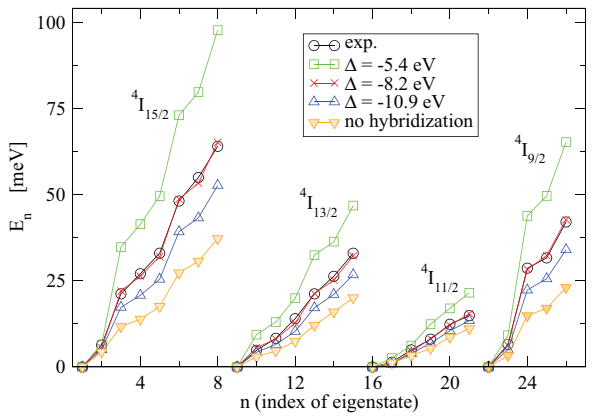

FIG. 8. (Color online) Er:$YAlO_3$. Energies of Er^{3+} eigenstates taken relative to the lowest energy of the multiplet. The experimental data were determined by Donlan and Santiago (Ref. 18) and Duan *et al.* (Ref. 1).

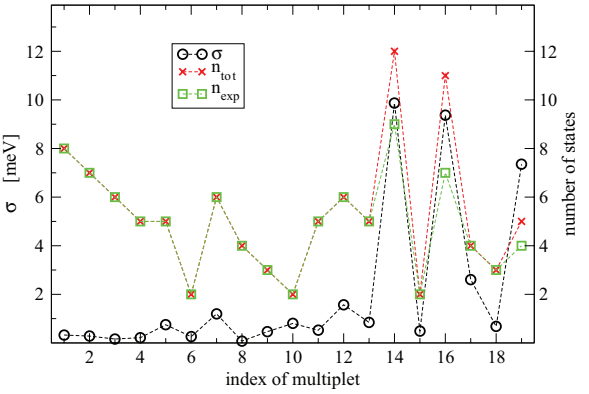

FIG. 9. (Color online) Er:$YAlO_3$. The mean square deviation σ of the experimental splittings and splittings calculated with $\Delta = -8.2$ eV (left vertical axis). The total number of levels in the set n_{tot} is denoted by crosses; the number of levels observed experimentally n_{exp} is denoted by squares (axis on the right). The experimental data were determined by Donlan and Santiago (Ref. 18) and Duan *et al.* (Ref. 1).

an ambiguity connected with numerous local minima of the minimization in the 14 dimensional space. Returning to the Er:$YAlO_3$ case (Fig. 9), in which the agreement between our calculation and the incomplete experimental multiplet splittings was significantly worse for the level sets 14, 16, and 19, we point out that assignment of the measured transitions is far from being unique. The present calculation may serve as a useful starting point for fitting of the optical spectra.

There are several limitations of the present method, which can be overcome with more or less expensive methods. Large multiplet separations, in particular near half filling of the $4f$ shell, may lead to a non-negligible multiplet dependence of the $4f$-ligand charge-transfer energies. It would lead to different hybridization contributions to CFP for different multiplets, an effect considered by the correlation crystal field method[21,22]. The present approach can deal with such a situation by using Δ corrected by multiplet splitting. Given that different multiplets of Nd^{3+}, Tb^{3+}, and Er^{3+} are well described by a single CFP set each, the multiplet dependence of CFP plays only a minor role in studied cases.

The restriction of the ligand states to those of the valence band is not always possible. In some cases the $f^n \rightarrow f^{n-1}d$ charge transfer may be relevant. The present method is readily

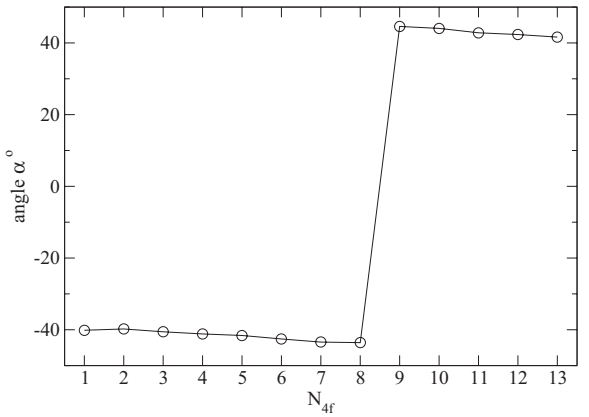

FIG. 10. Angle of rotation around orthorhombic c axis.

TABLE I. Comparison of absolute values of crystal field parameters calculated with the shift $\Delta = -8.2$ eV with those obtained by Duan *et al.* and Gruber *et al.* by least squares fit to optical spectra. All CFP are in units of cm^{-1}.

		$Nd:YAlO_3$		Tb in $TbAlO_3$		$Er:YAlO_3$	
k	q	Calc.	Expt.[a]	Calc.	Expt.[b]	Calc.	Expt.[a]
2	0	157	154	355	757	192	178
4	0	319	541	114	469	233	134
6	0	711	671	621	503	364	453
2	2	545	578	546	262	436	490
4	2	694	967	544	181	407	499
6	2	419	512	256	476	180	208
4	4	625	682	696	375	599	627
6	4	1566	1611	1096	1235	840	808
6	6	101	132	210	512	65	78

[a]Reference 1.
[b]Reference 2.

applicable with the Δ shift applied to the relevant states. In the most general situation the charge-transfer energy is small and the perturbative treatment of the $4f$-ligand hybridization is not justified. In such cases the hybridization and $4f$ interaction has to be treated simultaneously, either in a cluster calculation[23] or solving the quantum impurity problem.[24] In both cases, the Wannier construction including the ligand states explicitly can be used to construct the effective Hamiltonian. Nevertheless, the analysis of such Hamiltonian is much more demanding than the atomic calculation presented here.

The present approach can be implemented with any full potential electronic structure code. The only prerequisites are the possibility to eliminate the nonspherical part of the $4f$ self-interaction in the self-consistent calculation and the possibility to construct the Wannier orbitals.

VII. CONCLUSIONS

We have presented a method to calculate the crystal-field parameters for the $4f$ shells of rare-earth atoms from density functional theory with a single adjustable parameter Δ corresponding to the $4f$-ligand charge-transfer energy, which can be estimated from optical experiments. We were able to obtain the crystal-field splittings of rare-earth impurities in $YAlO_3$ within a few meV accuracy. The simplicity of the present method makes it a useful tool to compute optical, magnetic, and thermodynamical properties of rare-earth atoms away from the Kondo regime.

ACKNOWLEDGMENTS

The work was supported by Project No. 204/11/0713 of the Grant Agency of the Czech Republic and by the Deutsche Forschungsgemeinschaft through FOR1346.

APPENDIX: MANY-BODY PICTURE OF f-p HYBRIDIZATION

In order to illustrate the origin of the adjustable parameter Δ we resort to a simplified cluster model which includes the rare-earth ion surrounded by ligand atoms and treats the two-particle repulsion explicitly. Its Hamiltonian reads

$$\hat{H} = \sum_{i,j} h^{\rm at}_{ij} \hat{f}^\dagger_i \hat{f}_j + \frac{U}{2}\hat{N}_f(\hat{N}_f - 1) + \hat{W}_f + \sum_{i,k}(V_{ik}\hat{f}^\dagger_i \hat{p}_k + V_{ki}\hat{p}^\dagger_k \hat{f}_i) + \sum_k \epsilon_k \hat{p}^\dagger_k \hat{p}_k, \quad \text{(A1)}$$

where the operators $\hat{f}$ and $\hat{p}$ annihilate an electron in the $4f$ and the ligand orbitals, respectively. The first term represents the on-site (electrostatic) crystal field and the spin-orbit coupling in the $4f$ shell; the second and third term is the electron-electron interaction within the $4f$ shell split into the SU(N) symmetric U term and the rest $\hat{W}_f$, responsible for multiplet splitting. The fourth term describes the $4f$-ligand hybridization $\hat{V}$ and the last term describes the site energies of the ligand orbitals. In situations studied in this work the lowest valence state f^n is well separated from the excited states $f^{n+1}\underline{L}$ obtained by a charge transfer from ligand to the rare earth. We assume that average charge transfer energy $\Delta_{\rm fp} = E(f^{n+1}\underline{L}) - E(f^n)$, determined by the isotropic U part of the interaction and the average separation of the bare $4f$ and ligand levels, is large compared to its variation, due to the multiplet splitting ($\hat{W}_f$) and the distribution of ligand levels (ϵ_k), and treat $\Delta_{\rm fp}$ as a constant. We reduce the Hamiltonian (A1) to the f^n subspace. In the process the $4f$-ligand hybridization gives rise to corrections to the crystal field Hamiltonian $h^{\rm at}$. We restrict ourselves to the familiar second order perturbation. The first and third terms of (A1) are unchanged, and the second term turns into a constant. The correction due to hybridization amounts to

$$\langle\alpha|\hat{H}_{\rm hyb}|\beta\rangle = -\sum_\gamma \frac{\langle\alpha|\hat{V}|\gamma\rangle\langle\gamma|\hat{V}|\beta\rangle}{\Delta_{\rm fp}}, \quad \text{(A2)}$$

where α and β are Slater determinants from the f^n subspace and γ belongs to the $f^{n+1}\underline{L}$ subspace. The only nonzero elements of $H_{\rm hyb}$ are the diagonal ones and elements between states that differ by transfer of a single electron between two orbitals, i.e., $H_{\rm hyb}$ is a correction to the one-particle part of the atomic Hamiltonian. Equation (A2) yields for diagonal elements

$$\begin{aligned}\langle\alpha|\hat{H}_{\rm hyb}|\alpha\rangle &= -\frac{1}{\Delta_{\rm fp}}\sum_{k,\ i\ \text{empty}} V_{ik}V_{ki} \\ &= E_0 + \frac{1}{\Delta_{\rm fp}}\sum_{k,\ i\ \text{full}} V_{ik}V_{ki} \\ &= E_0 + \frac{1}{\Delta_{\rm fp}}\sum_i\sum_k V_{ik}V_{ki}\langle\alpha|\hat{f}^\dagger_i\hat{f}_i|\alpha\rangle, \quad \text{(A3)}\end{aligned}$$

where $E_0 = -\frac{1}{\Delta_{\rm fp}}\sum_{i,k} V_{ik}V_{ki}$ is a constant shift. To evaluate the off-diagonal elements we use the Slater determinants

$$\begin{aligned}|\alpha\rangle &= \hat{f}^\dagger_j\hat{f}_i|N\rangle \\ |\beta\rangle &= |N\rangle \\ |\gamma\rangle &= \hat{f}^\dagger_j\hat{p}_k|N\rangle,\end{aligned}$$

where $|N\rangle$ is a state from the f^n subspace. In this basis we get

$$\begin{aligned}\langle\alpha|\hat{H}_{\rm hyb}|\beta\rangle &= -\frac{1}{\Delta_{\rm fp}}\sum_k V_{jk}V_{ki}\langle N|\hat{f}_i^\dagger\hat{f}_j\,\hat{p}_k^\dagger\hat{f}_i\;\hat{f}_j^\dagger\hat{p}_k|N\rangle\\ &\quad\times\langle N|\hat{p}_k^\dagger\hat{f}_j\,\hat{f}_j^\dagger\hat{p}_k|N\rangle\\ &= -\frac{1}{\Delta_{\rm fp}}\sum_k V_{jk}V_{ki}\langle N|\hat{f}_i^\dagger\hat{f}_j\,\hat{f}_i\;\hat{f}_j^\dagger|N\rangle\langle N|N\rangle\\ &= \frac{1}{\Delta_{\rm fp}}\sum_k V_{jk}V_{ki}\\ &= \frac{1}{\Delta_{\rm fp}}\sum_k V_{jk}V_{ki}\langle\alpha|\hat{f}_j^\dagger\hat{f}_i\,|\beta\rangle. \qquad \text{(A4)}\end{aligned}$$

Equations (A3) and (A4) describe the correction to the crystal-field Hamiltonian arising from the hybridization to ligands. Including this correction and omitting irrelevant constants the effective Hamiltonian for the f^n subspace reads

$$\hat{H} = \sum_{i,j}\left(h_{ij}^{\rm at} + \sum_k \frac{V_{ik}V_{kj}}{\Delta_{\rm fp}}\right)\hat{f}_i^\dagger\hat{f}_j + \hat{W}_f. \qquad \text{(A5)}$$

Note that the identical form of the correction would be obtained in a noninteracting system with $\Delta_{\rm fp}$ playing the role of the difference of one-particle levels $\epsilon_f - \epsilon_p$. The shift Δ of the p levels introduced in our computational procedure thus mimics the effect of the electron-electron repulsion within the $4f$ shell:

$$\Delta = (\epsilon_f - \epsilon_p) - \Delta_{fp}. \qquad \text{(A6)}$$

The physical meaning of the energy separation of the f and p states after the shift is the charge-transfer energy, i.e., energy cost of moving and electron from ligand to the rare-earth ion, in the real interacting system. The stability of the f^n rare-earth valence state implies that $\Delta_{\rm fp}$ is always positive. Because of the interacting nature of the system $\Delta_{\rm fp}$ is not directly related to the positions of $4f$ and O p peaks in photoemission experiment, which may even have reversed order. Similar considerations apply to excursions to $f^{n-1}d$ states, which have, however, a much smaller amplitude.

*novakp@fzu.cz

[1] C. K. Duan, P. A. Tanner, V. N. Makhov, and M. Kirm, Phys. Rev. B **75**, 195130 (2007).

[2] J. B. Gruber, K. L. Nash, R. M. Yow, D. K. Sardar, U. V. Valiev, A. A. Uzokov, and G. W. Burdick, J. Lumin. **128**, 1271 (2008).

[3] S. Hufner, *Optical Spectra of Transparent Rare Earth Compounds* (Academic, New York, 1978).

[4] W. T. Carnall, G. L. Goodman, K. Rajnak, and R. S. Rana, J. Chem. Phys. **90**, 3443 (1989).

[5] B. G. Wybourne, *Spectroscopic Properties of Rare Earth* (Interscience, New York, 1965).

[6] P. Novák, *Rare Earth: New Research* (Nova Science Publishers, Inc., in print).

[7] C. Rudowicz and J. Qin, Phys. Rev. B **67**, 174420 (2003).

[8] P. Blaha, K. Schwarz, G. K. H. Madsen, D. Kvasnicka, and J. Luitz, *WIEN2k, An Augmented Plane Wave + Local Orbitals Program for Calculating Crystal Properties*, edited by Karlheinz Schwarz (Techn. Universität, Wien, Austria, 2001).

[9] J. P. Perdew, K. Burke, and M. Ernzerhof, Phys. Rev. Lett. **77**, 3865 (1996).

[10] R. Diehl and G. Brandt, Mater. Res. Bull. **10**, 85 (1975).

[11] A. Bombik, B. Lesniewska, J. Mayer, and A. W. Pacyna, J. Magn. Magn. Mater. **257**, 206 (2003).

[12] J. Kuneš, R. Arita, P. Wissgott, A. Toschi, H. Ikeda, and K. Held, Comput. Phys. Commun. **181**, 1888 (2010).

[13] A. A. Mostofi, J. R. Yates, Y.-S. Lee, I. Souza, D. Vanderbilt, and N. Marzari, Comput. Phys. Commun. **178**, 685 (2008).

[14] L. Hu, M. F. Reid, Ch-K. Duan, S. Xia, and M. Yin, J. Phys.: Condens. Matter **23**, 045501 (2011).

[15] P. Novák and M. Diviš, Phys. Status Solidi B **244**, 3168 (2007).

[16] S. Edwardsson and D. Aberg, Comput. Phys. Commun. **133**, 396 (2001).

[17] A. A. Kaminskii, *Laser Crystals* (Springer-Verlag, Berlin, 1981).

[18] V. L. Donlan and A. A. Santiago, J. Chem. Phys. **57**, 4717 (1972).

[19] E. Rogers, P. Dorenbos, and E. van der Kolk, New J. Phys. **13**, 093038 (2011).

[20] P. Wissgott, J. Kuneš, A. Toschi, and K. Held, Phys. Rev. B **85**, 205133 (2012).

[21] B. R. Judd, Phys. Rev. Lett. **39**, 242 (1977).

[22] R. G. Denning, A. J. Berry, and C. S. McCaw, Phys. Rev. B **57**, R2021 (1998).

[23] M. W. Haverkort, M. Zwierzycki, and O. K. Andersen, Phys. Rev. B **85**, 165113 (2012).

[24] J. Kuneš, V. I. Anisimov, A. V. Lukoyanov, and D. Vollhardt, Phys. Rev. B **75**, 165115 (2007).